Hydrology and
Earth System
Sciences
Discussions

Seasonally varied hillslope and groundwater contributions to streamflow in a glacial till and fractured sedimentary bedrock dominated Rocky Mountain watershed.

Sheena A. Spencer[1], Axel E. Anderson[1,2], Uldis Silins[1], Adrian L. Collins[3]

5 [1]Department of Renewable Resources, University of Alberta, Edmonton, T6G 2G7, Canada
[2]Alberta Agriculture and Forestry, Government of Alberta, Edmonton, T5K 1E4, Canada
[3]Sustainable Agriculture Sciences, Rothamsted Research, North Wyke, Okehampton, EX20 2SB, United Kingdom

Correspondence to: Sheena A. Spencer (sheena.spencer@ualberta.ca)

Abstract. Whereas a lack of streamflow response to significant forest disturbance (e.g., forestry, wildfire, and insect
10 infestation) has been observed at multiple locations in the Canadian Rocky Mountains, a region with sedimentary bedrock overlain by glacial till, mechanisms governing this lack of change remain unclear. Some inferences can be drawn from conceptualizations of runoff generation (e.g., runoff thresholds and hydrologic connectivity) in physically similar watersheds, although much of the focus has been on rainfall-runoff dynamics. Thus, there is a need to describe runoff generation in this snow-dominated area to interpret how forest disturbance may impact streamflow quantity for downstream users. Stream water
15 and source water (snow, rain, hillslope groundwater, till groundwater, bedrock groundwater and seeps) were sampled in four sub-watersheds (Star West Lower, Star West Upper, Star East Lower and Star East Upper) in Star Creek, SW Alberta. Principal component analysis was used to determine the relative dominance and timing of source water contributions to streamflow over the 2014 and 2015 hydrologic seasons. An initial displacement of old water stored in the hillslope over winter occurred at the onset of snowmelt, before the stream responded significantly. This was followed by a dilution effect as snowmelt saturated the
20 landscape, recharged groundwater, and connected the hillslope to the stream. Fall baseflows were dominated by either hillslope groundwater or bedrock groundwater in Star West. Conversely, in Star East, stream water was similar to hillslope water in August but was unlike the measured sources in September and October. Temperature and chemical signatures of groundwater seeps suggest highly complex subsurface flow pathways. Hydrologic resilience in the Rocky Mountain eastern slopes may be, in part, due to these complex subsurface pathways in combination with the slow release of groundwater from glacial till.
25

1 Introduction

Forest disturbance from wildfire, pine beetle infestation, or forest harvesting removes the forest canopy increasing the total
30 precipitation that reaches the forest floor (Williams et al., 2019; Burles and Boon, 2011; Boon, 2012; Varhola et al., 2010)
often altering the dominant flow pathways, increasing streamflow quantity and changing the timing of flows in forested
watersheds (Stednick, 1996; Scott, 1993; Winkler et al., 2017). However, large variability has been observed in streamflow
responses following disturbance due to differences in disturbance type, vegetation type, precipitation regimes, and soil
moisture storage (Brown et al., 2005; Stednick, 1996). Some studies have reported little, if any, change in streamflow following
35 disturbance (Williams et al., 2015; Harder et al., 2015; Goodbrand and Anderson, 2016; Andres et al., 1987) but the
mechanisms or features potentially responsible for the lack of flow response remain unclear. Watershed resilience, when a
watershed maintains a similar form and function following forest disturbance (Creed et al., 2011), has been used to explain the
lack of change in streamflow following disturbance (Harder et al., 2015). Watersheds exhibiting resilience might be associated
with a large storage capacity and complex subsurface flow pathways (Harder et al., 2015) where water can be stored for months
40 or years and be subsequently released to the stream gradually thereby buffering the flow response of watersheds from
disturbance (Creed et al., 2011).

High bedrock permeability is a watershed feature that has been associated with the slow release of stored water to streams
during baseflow (Uchida et al., 2006; Liu et al., 2004; Pfister et al., 2017), thereby potentially influencing the hydrological
resilience. Uchida et al. (2006) reported that a watershed with greater bedrock permeability had larger aquifer storage, and the
45 subsequent release of stored water maintained baseflow later in the year. Similarly, Liu et al. (2004) showed that the recession
limb of the annual hydrograph in the Colorado front range Rocky Mountains was driven by baseflow released from fractured
bedrock. Deep soils and till deposits with large storage capacities have also been shown to sustain baseflows during drier
periods (Floriancic et al., 2018; Shanley et al., 2015). Deep sediment deposits in the Poschiavino watershed, in Switzerland,
were associated with larger storage capacity and higher winter baseflows compared to watersheds with shallow sediment
50 deposits (Floriancic et al., 2018). Similarly, deep basal till in Sleepers River watershed in Vermont was associated with large
storage capacity and low permeability that promoted extended maintenance of baseflow (Shanley et al., 2015).

While these studies illustrate the influence of bedrock, deep soils, or till on baseflows, few studies have explored the
combination of these storage zones on streamflow contributions (Burns et al., 1998; Dalke et al., 2012; Spencer et al., 2019).
Burns et al. (1998) characterized the difference in deep (bedrock) and shallow (soils and till) flow systems in the Catskill
55 Mountains in New York, a region with both glacial till and permeable sedimentary bedrock. Baseflow was maintained by
discharge from perennial springs, which originated from bedrock fractures, rather than contributions from the soil and till flow
system (Burns et al., 1998). Similarly, precipitation-runoff relationships in Alberta's Rocky Mountains indicated that runoff
generation is complicated by the interaction of two storage zones – soil and till storage and bedrock storage (Spencer et al.,
2019) where coupled flow and tracer approaches would be needed to reduce uncertainty in estimated flow contributions from
60 each storage zone. Others have also shown the importance of groundwater contributions to streamflow in alpine watersheds in

the Rocky Mountains (Hood and Hayashi, 2015; McClymont et al., 2010). However, due to the highly heterogeneous nature of glacial till, more research is needed to differentiate between baseflow contributions from glacial till and bedrock storage sources.

Chemical signatures of source water (e.g., glacial till groundwater, bedrock groundwater, soil water, and precipitation) and stream water can be used to determine which sources are contributing to streamflow during different flow conditions using end-member mixing (Christophersen and Hooper, 1992). Accordingly, the objectives of this study were to: 1) characterize how sources of stream water (precipitation, soil water, hillslope groundwater, till groundwater, bedrock groundwater, and seeps) vary spatially across four sub-watersheds of a Rocky Mountain watershed and temporally from spring snowmelt to fall low flows, and; 2) determine the relative contributions of source water to the stream from spring to fall for each sub-watershed. Two adjacent geologically similar watersheds were compared to explore the relative variation in stream water sources across key physiographic zones (higher elevation alpine/sub-alpine vs lower elevation upper montane) that were evident within Star Creek watershed. This study should help inform the current conceptualization of runoff generation in northern Rocky Mountain watersheds, thereby providing new understanding of the potential factors influencing watershed resilience to close a critical evidence gap.

2 Study Site

Star Creek watershed (10.4 km^2; Figure 1) is located in the eastern slopes of Canada's Rocky Mountains; a region with fractured sedimentary bedrock overlain by glacial till. Area-weighted average precipitation is 950 mm, with 50-60 % in the form of snow. Soils are Eutric Brunisols (Can. Soil Classification, or Eutric Cambisols in Food and Agriculture Organization system) approximately 1 m deep, on average. Unsorted and uncompacted glacial till is 3 m deep, on average, with some clay-rich layers distributed unevenly throughout the watershed. Sedimentary geologic formations are primarily composed of shale and sandstone and are highly fractured due to folding and faulting (AGS, 2004).
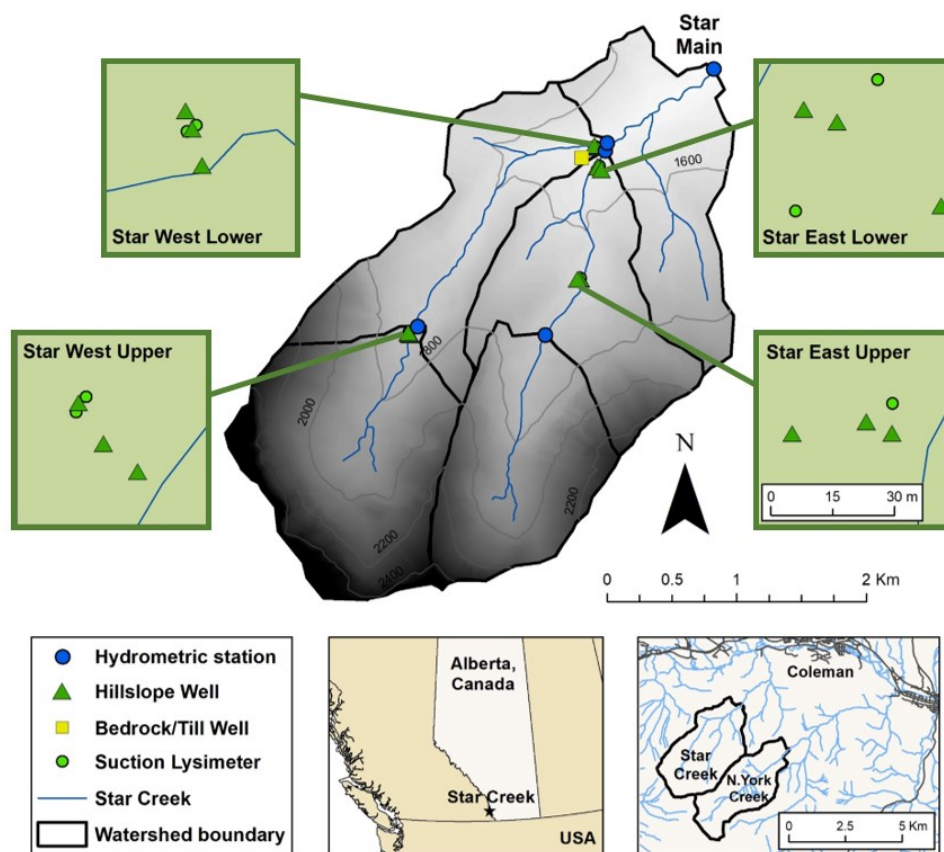
There are two main sub-watersheds, Star East (3.9 km^2; 1537-2628 m above sea level) and Star West (4.6 km^2; 1540-2516 m above sea level). Unvegetated talus slopes beneath exposed bedrock form the upper portion of alpine zones in both sub-watersheds. Star West has a larger alpine region with till deposits that includes a narrow marshy area proximal to the stream that holds water throughout the summer and drains into the main channel that is primarily bedrock in the upper reaches. The Star East alpine region is smaller and more constricted than in Star West (Figure 2) and is comprised mostly of a grassy meadow with the stream originating from springs where the water table reaches the soil surface and is incised in colluvium with large boulders. In the lower reaches, streams in both sub-watersheds are composed of a series of step-pools incised in alluvium and colluvium where the lower sub-alpine and upper Montane zones are dominated by sub-alpine fir (*Abies lasiocarpa*) and Englemann spruce (*Picea Englemannii*) above lodgepole pine (*Pinus contorta*) dominated forests in lower reaches (Dixon et al., 2014; Silins et al., 2009).

Two historical streamflow gauging sites exist in each sub-watershed – a lower site (Star West Lower (SWL) and Star East Lower (SEL)) near the confluence of the two sub-watersheds (1540 m above sea level) and an upper site (Star West Upper (SWU) and Star East Upper (SEU)) located at approximately 1690 m above sea level in the alpine/sub-alpine transition zone.

95

Figure 1: Star Creek watershed. Suction lysimeter and hillslope groundwater well locations are magnified in green boxes.

Figure 2: Star East (left) and Star West (right) sub-watersheds. The Star East alpine area is more constrained and smaller than the Star West alpine area. Both sub-watersheds have steep headwalls with talus slopes in the alpine zone.

3 Methods

3.1 Stream water chemistry

Stream water samples were collected from the four streamflow gauging stations (SEL, SEU, SWL, SWU; Figure 1) every two weeks from April to October, in 2014 and 2015, to capture the full range in streamflow chemistry over the hydrologically active period. One litre plastic bottles were triple rinsed prior to sample collection. Samples were analyzed for major cations and anions (Na^+, Mg^{2+}, Ca^{2+}, K^+, Cl^-, SO_4^{2-}) and silica (Si as SiO_2) in the Biogeochemical Analytical Service Laboratory (University of Alberta). An inductively coupled plasma-optical emission spectrometer (Thermo Scientific ICAP 6300) was used to measure Na^+, Mg^{2+}, Ca^{2+}, K^+ with analytical precision of 1.9 %, 3.0 %, 1.9 %, and 2.4 %, respectively. An ion chromatograph (Dionex DX600 and Dionex ICS 2500) was used to measure Cl^- and SO_4^{2-} with analytical precision of 2.4 % and 3.1 %. Flow injection analysis (Lachat QuikChem 8500 FIA automated ion analyzer) was used to measure Si with analytical precision of 3.4 %.

3.2 Source water chemistry

Stream water sources were a priori hypothesized to be rain, snowmelt, soil water, hillslope groundwater, and groundwater seeps. All source water samples were collected in triple rinsed (with source water) 50 ml plastic vials and analyzed with the same methods as the stream water samples to support application of end-member mixing analysis. Source water collection and sampling methods are detailed below.

3.2.1 Rainfall and snowmelt

Rain samples were collected in a clean bucket that was rinsed with deionized water. Buckets were placed in open areas throughout the watershed or in the nearby townsite (Coleman, AB; within approximately 8 km of Star Creek watershed) after a rainstorm began. Locations were chosen opportunistically depending on storm timing and site access. Samples were collected at the end of the day or once there was enough water in the bucket to sample, to prevent changes in chemical composition due to dry deposition of dust or evaporation. Five, four, and three samples were collected throughout the summers of 2013, 2014, and 2015, respectively. The difficulty of capturing large convective storms and the large frequency of storms less than 5 mm (Williams et al., 2019) prevented the collection of more rainfall samples.

Eleven snowmelt samples were collected from sub-alpine regions of Star Creek and North York Creek (an adjacent watershed, Figure 1) throughout spring and early summer in 2014. Three additional samples were collected in spring 2015 but mid-winter melt of snowpacks hindered the collection of more snowmelt samples. Eavestroughs, 3 m in length, were installed perpendicular to the stream with a small overhang off the edge of the hillslope in Star Creek and North York Creek watersheds prior to snow accumulation. Samples were collected directly from snowmelt troughs and snow bridges with clearly visible melt. Snowmelt was sampled, instead of the snowpack, to better reflect the meltwater signature during the snowmelt period (Johannessen and Henriksen, 1978).

3.2.2 Soil water

Suction lysimeters were installed between 30-60 cm depth using a hand auger in two locations near the toe of the hillslope in each sub-watershed in early spring 2014 (2015 for SEU; Figure 1). Suction lysimeters consisted of a 0.5 Bar ceramic cup and 38.1 mm PVC pipe to ensure ample water was collected for chemical analyses. Water from the suction lysimeter was sampled using a hand pump every two weeks between April and October in 2014 and 2015. Suction lysimeters were pumped dry following sampling and pressure was applied. Thus, soil water was composed of water that was able to pass through the ceramic cup over the two-week period until the lysimeter was at equilibrium pressure with the surrounding soil. Shallow depths were targeted with the intention to collect the unsaturated soil water above the saturated zone in the hillslope, which was sampled separately.

3.2.3 Hillslope groundwater

Hillslope wells were installed with a shovel or hand auger to depth of refusal or maximum auger depth (1.5 m) near the hydrometric gauging stations at SEL, SEU, SWL and SWU (Figure 1). A site was added at SEU at the end of the summer in 2014, whereas the other sites were established during summer 2013. Wells were installed in three locations at each site: riparian, toe slope, and hillslope positions to determine the full range in hillslope groundwater. Well depths ranged between 0.5 m (riparian wells) and 1.6 m. Wells were purged using a hand pump prior to sampling. Samples were collected approximately every two weeks, as available, between April and October in 2014 and 2015. Samples from the upper hillslope wells were generally only obtained during the snowmelt or high flow period; these wells were often dry during late summer. Riparian and toe slope wells contained water for all or most of the year, respectively.

3.2.4 Groundwater seeps

At the onset of this research, lack of access to backcountry sites restricted the installation of deep bedrock or till groundwater wells in upper sub-watersheds. Rather, groundwater seeps were used to characterize the possible range in groundwater signatures (both bedrock and till groundwater) within Star Creek. Seeps are defined here as areas of visible water seeping from hillslopes proximal to the stream or from small wetland areas further from the stream that form small tributaries or rivulets that flow into the stream. The east and west forks were surveyed from the confluence with the main stem to the stream origins in the alpine area in July 2013; 25 visible seeps were identified. Samples were collected during three flow conditions: high flow (May/June), recession flow (mid-July), and baseflow (early September prior to fall rains), in both 2014 and 2015. Water temperature was also measured during sample collection to aid in differentiating between deep bedrock groundwater, till groundwater and hillslope groundwater.

3.2.5 Bedrock and till groundwater

160   Preliminary end-member mixing analysis showed that a water source was missing from those initially collected (above) highlighting the need to characterize deeper groundwater. Due to monetary and access limitations, a single borehole was drilled to 12 m depth (15.2 cm in diameter) in the topographic ridge between SEL and SWL (approx. 500 m upstream from gauging sites) in October 2015 (Figure 1). Two wells were installed in the borehole, one well in a water-baring formation in the bedrock at 11 m depth, and a second well in the glacial till deposits at 4.5 m depth, to characterize the differences in bedrock and till

165   groundwater chemistry. Both wells had screens that were 1.5 m in length. Sand was used to backfill the borehole around the screened section of the bedrock groundwater well and was capped with bentonite clay. Local material removed during drilling was used to backfill the borehole up to the till layer. The same method of back filling (sand, bentonite clay, local material) was used for the till groundwater well. Bedrock and till wells were sampled every two to four weeks in 2016 and 2017. Water in the till well was purged until dry prior to sampling. Water in the bedrock well was purged for 2-5 minutes prior to sampling

170   because the recharge rate was faster than the pump rate. Water table depth and temperature were measured continuously with pressure transducers (HOBO U20, Onset Computer Corp., Bourne, MA, USA) at 10-minute intervals.
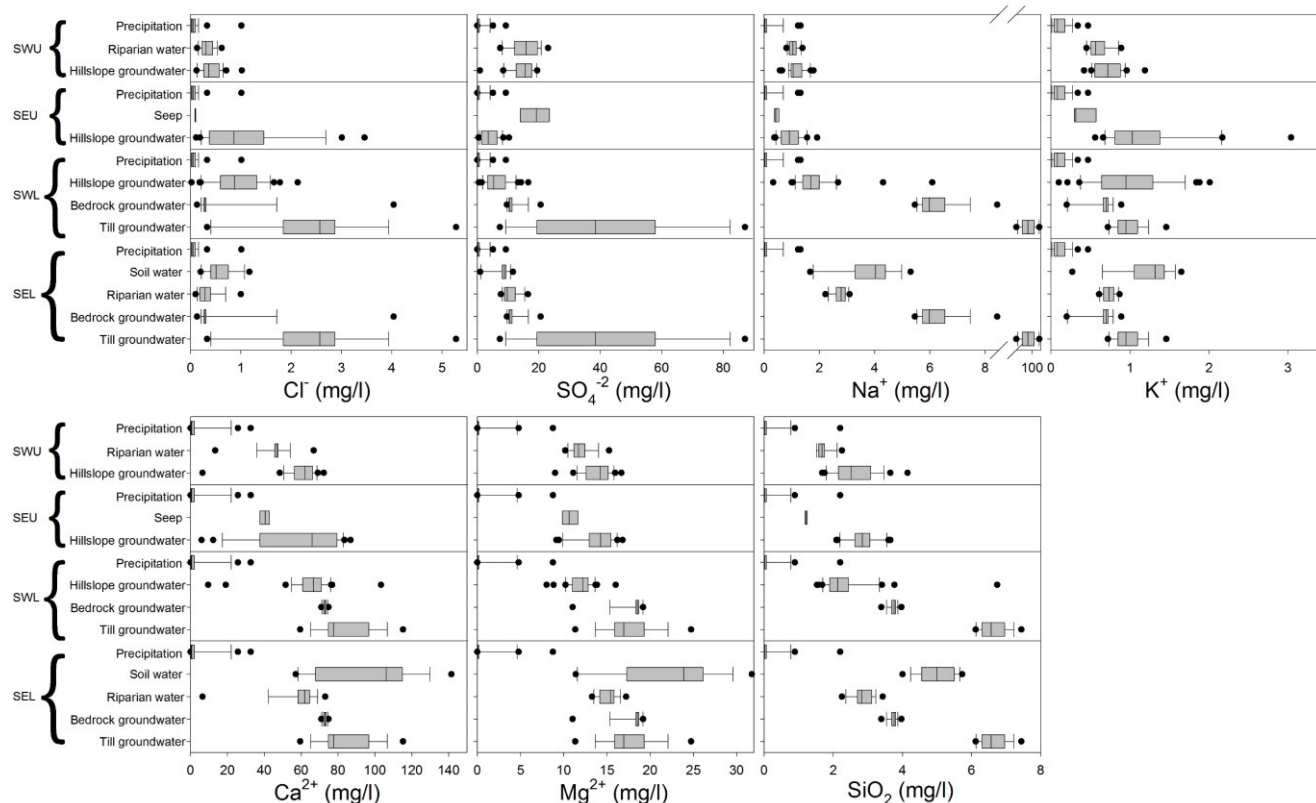

Figure 3: Box plots for Star West Upper (SWU), Star East Upper (SEU), Star West Lower (SWL), and Star East Lower (SEL) showing the ranges in chemistry for potential sources.

175   High concentrations of Na$^+$, Cl$^-$, and SO$_4{}^{2-}$ in till groundwater (Figure 3) and large variability between years suggested that the till groundwater well was likely contaminated by the bentonite clay used to backfill and seal between layers (Remenda and van der Kamp, 1997). Slow recharge rates (and therefore, low hydraulic conductivity) of glacial till prevented the removal of three pipe volumes when sampling and the corresponding low hydraulic conductivity resulted in little flushing of bentonite contaminants. Faster recharge rates (and therefore, higher hydraulic conductivity) of the bedrock groundwater would aid in

180   better flushing of bentonite contaminants which would reduce the effects on bedrock groundwater chemistry (Remenda and van der Kamp, 1997). As a result, the till groundwater samples were not included in the analyses herein; however, water table depths and water temperature dynamics could still be used to understand the differences between till and bedrock groundwater responses and their roles in runoff generation.

4 Data Processing

185   End-member mixing analysis (EMMA) was used to visualize multi-variate source water and stream chemistry by reducing the dimensionality of the data with principal component analysis (PCA; Christophersen and Hooper, 1992). The key assumptions for EMMA are: 1) the tracers are conservative; 2) the mixing process is linear; 3) source chemistry does not change temporally or spatially over the period or area studied (Inamdar, 2011; Hooper, 2003), and; 4) all sources have been identified and have the potential to contribute to streamflow. In addition, there were multiple subjective decisions required prior to running

190   EMMA, such as choosing tracers/ions and defining sources. Two methods were used to determine if tracers were appropriate to use in the analysis. A matrix of bivariate plots of stream chemistry data (ion concentrations), used most commonly in geographical hydrograph separations, was used to determine if ions were conservative in nature (Hooper, 2003). The tracer variability ratio (TVR), used most commonly in sediment source apportionment studies, was used to determine if the difference in ion concentrations between groups was larger than the variation within a source group (Pulley et al., 2015). The TVR was

195   calculated for each tracer pair and compared between each group as the percent difference between source group median divided by the average coefficient of variation between group pairs (Pulley et al., 2015). TVR should be greater than 2 to be considered appropriate for use in mixing calculations (Pulley and Collins, 2018), although depending on the dataset in question, a greater threshold may be adopted to make the tracer selection more stringent and to help reduce the numbers of tracers included in further data processing.

200   Box and whisker plots and linear discriminant analysis (LDA) were used to remove the subjectivity of defining sources (Ali et al., 2010; Pulley and Collins, 2018). Box and whisker plots were used as a visual means of discriminating between sources. LDA was then used to determine if the combined sources exhibited sufficiently robust statistical separation (Pulley and Collins, 2018). Other statistical classification methods, such as hierarchical clustering or k-means clustering, were not appropriate because source categories were known a priori. The data were processed using LDA in the MASS ('lda' function; Venables and Ripley, 2002) and klaR ('stepwise' function; Weihs et al., 2005) packages in R (R Core Team, 2014). The 'stepwise'

function was used with the 'backwards' direction in an attempt to maintain the most tracers; 'lda' method, and 'ability to separate' criterion.

After the sources were characterized, the stream water was processed using principal component analysis (PCA; 'prcomp' function in R; R Core Team, 2014) as a method of dimensionality reduction to create a two-dimensional (2D) mixing space

210 (Christophersen and Hooper, 1992). Stream water was standardized (subtracting the mean and dividing by the standard deviation for each sampling point), for each tracer, to create equal variance between chemical components and used to create a correlation matrix. PCA was conducted on the correlation matrix to calculate eigenvectors and eigenvalues. Standardized stream water was then projected into the end member mixing-space by multiplying by eigenvectors. Ideally, two principal components (PCs) explained most of the variation in the data and were used to generate a 2D mixing space, which corresponds

215 to three sources in EMMA (Hooper, 2003). Other studies have used the 'Rule of 1' to determine how many dimensions, and therefore sources, should be used to create the mixing space (Ali et al., 2010; Barthold et al., 2011). For this study, the mixing space was set to two dimensions for ease of visualization but used all appropriate sources as presented by Inamdar et al. (2013) to provide a full description of potential source contributions. Source water was then standardized using stream water means and standard deviations for each ion and projected into the 2D mixing space as defined by the stream water (Christophersen

220 and Hooper, 1992; Hooper, 2003). Stream water sources should create an outer boundary or polygon around all stream water samples if all sources were correctly identified and adequately sampled.

5 Results

5.1 Tracer and source water group selection

Bivariate plots were created and TVR was calculated to determine which tracers were appropriate for use in EMMA. Pearson

225 correlation coefficients were calculated between all stream bivariate plots for stream water at each sub-watershed (Figure 4). These showed that all tracers exhibited acceptable linear trends with at least one other tracer (Pearson's r > 0.5) and were thereby likely conservative in nature. Average TVR for almost all tracers at all sites (exception Si at SW and SE) were below 2, which suggested that the within-group variation exceeded the between-group variation and were considered unacceptable. As a result, rather than calculating mixing ratios or percent contributions on the basis of an un-mixing routine, trends in stream

230 water distribution were described in relation to source water dynamics and runoff processes, as suggested by Inamdar et al. (2013).

The a priori classification of water sources was rain, snowmelt, soil water, riparian water, toe slope water, upper hillslope water, groundwater seeps and bedrock groundwater; however, box and whisker plots showed that the distribution of rain and snowmelt were similar as well as the distribution of soil water, riparian water, toe slope water, and hillslope water for most

235 sites. Final source water groups (Figure 3) are described below for each sub-watershed. LDA plots indicated that LD1 and LD2 explained 88.5 % and 11.5 %, 95.3 % and 4.7 %, 81.1 % and 15.5 %, and 77.6 % and 22.4 % of the variance of the centroids for SWL, SWU, SEL, and SEU sites, respectively. Stepwise analyses were also used in attempt to reduce the

redundancy of the tracers and to ensure that samples were well separated; on this basis, 99.7 %, 91 %, 98.6 %, and 99.9 % of

samples were well separated in SWL, SWU, SEL, and SEU, respectively. In all sites, all tracers were retained to maximize the

240 ability to distinguish between the source groups. Overall, these results support the conclusion that there was good separation

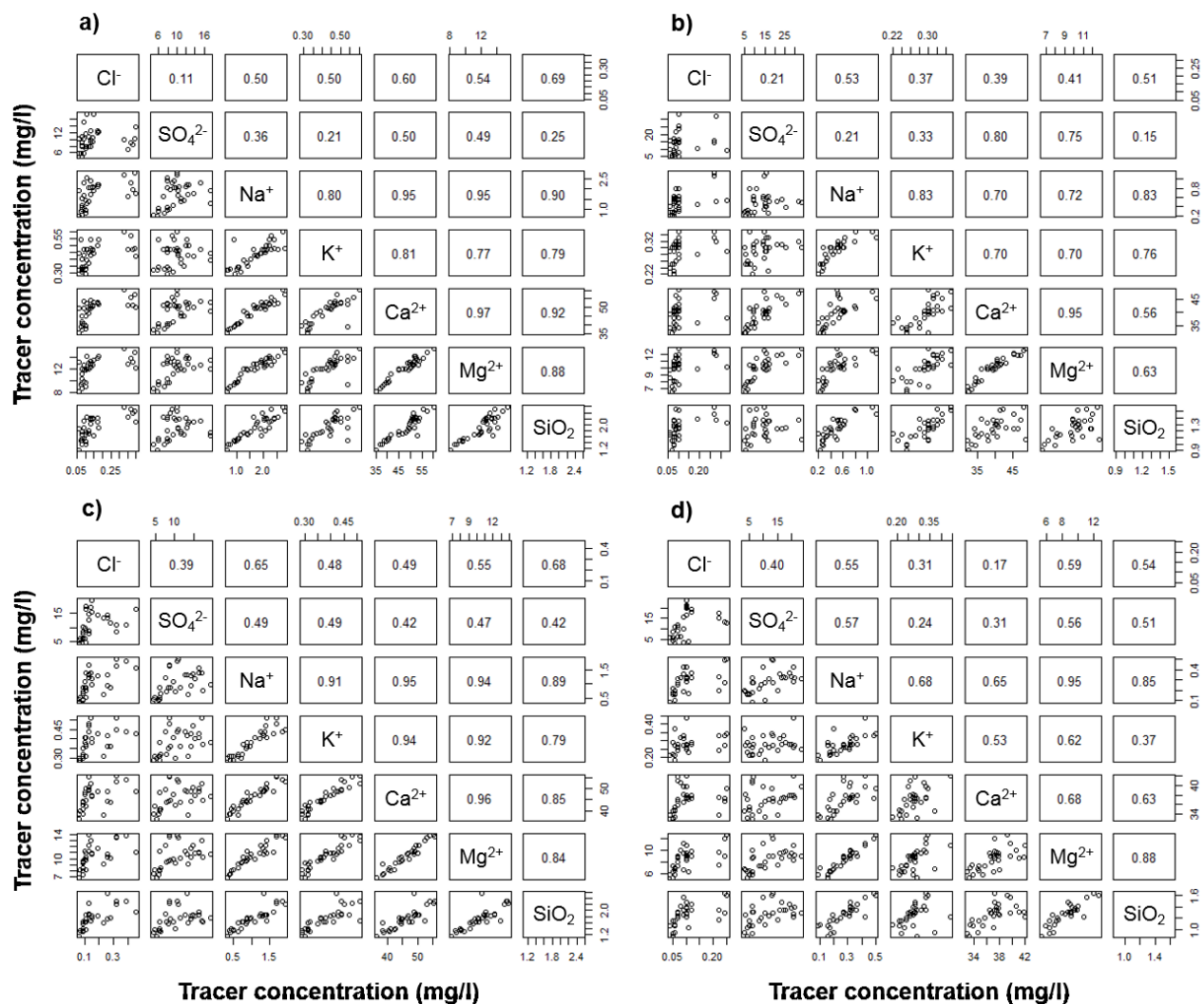between source water groups as re-categorized for the individual sites.

Figure 4: Bivariate plots of stream water chemistry at a) Star East Lower, b) Star East Upper, c) Star West Lower and d) Star West Upper. Top half of plots represents the Pearson's correlation coefficient (r) for the linear relation between each solute.

245 Groundwater seeps were sampled in leu of bedrock or till groundwater wells to characterize the variability in the chemical

signature of groundwater throughout Star Creek. The ion concentrations of the groundwater seeps were not chemically distinct

because they were generally similar to stream water or hillslope groundwater in the PCA analyses (data not shown). However,

examination of groundwater seep temperatures from spring to fall revealed that some seeps had consistently cool temperatures

and others had larger fluctuations in temperature. This suggests that some seeps were potentially groundwater-fed and others

250 were fed by shallow subsurface water, respectively. For example, in SEL, the temperature of a groundwater seep ranged between 2.2-3.7 °C throughout the summer, which is indicative of a bedrock groundwater source because the temperature range was muted and was largely not influenced by radiative warming (Taniguchi, 1993). Similarly, in SEU, the temperature of a groundwater seep ranged from 2.5-3.5 °C, also indicating a bedrock groundwater source. Temperatures in the till groundwater well ranged between 2.7-9.7 °C and the bedrock groundwater ranged between 5.1-5.8 °C. Both groundwater

255 seeps mentioned above had low variability like bedrock groundwater but were cooler suggesting a deeper bedrock groundwater source than in the well. Temperatures of the other groundwater seeps were more similar to bedrock groundwater, ranging from 3.6-5.4 °C, and others were more similar to surface water sources, ranging from 3.8-9.4 °C.

5.2 Source water characterization

5.2.1 Star West Lower

260 Sources were grouped as precipitation (rain and snow), hillslope groundwater (soil water, riparian water, and toe slope water), and bedrock groundwater and plotted in PCA mixing space (Figure 5). Minimal variation across all precipitation samples (standard deviation (SD) of 2.4 and 1.1 for PC1 and PC2, respectively) and overlap of snow and rain samples in the mixing
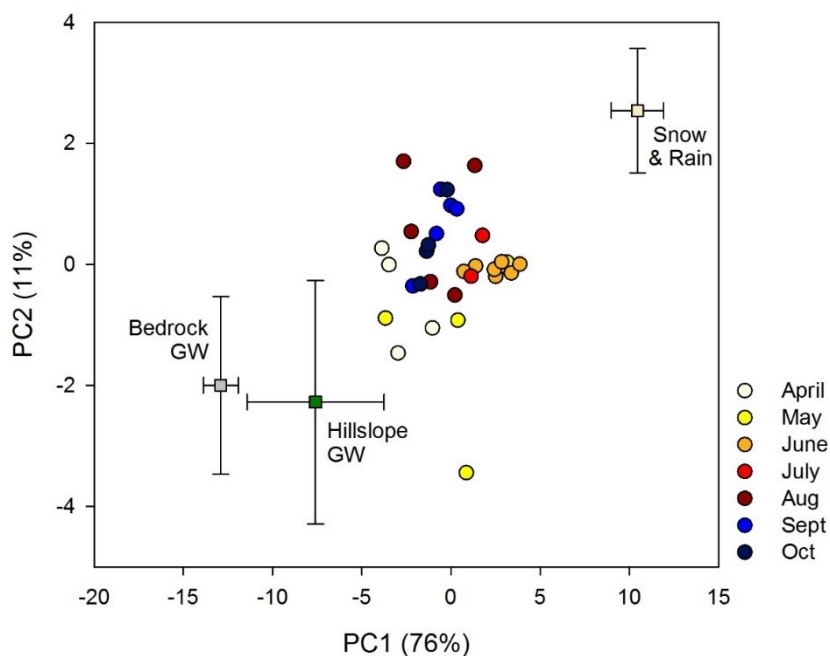

Figure 5: Star West Lower stream water chemistry from April to October in 2-D mixing space, which was derived from principal
265 **component analysis. Source water (precipitation, hillslope groundwater, and bedrock groundwater) was projected into the stream water mixing space. PC1 and PC2 represent the first and second principal components, which explain 87 % of the variation in stream water. Error bars represent the standard deviation of the source waters for PC1 and PC2.**

space confirmed that it was appropriate to aggregate all samples (snow and rain) taken across all sites (Star Creek, York Creek, and Coleman). Hillslope groundwater exhibited greater variation across samples (SD of 3.8 and 2.0 for PC1 and PC2,

270 respectively), but no clear temporal pattern was observed. Bedrock groundwater chemistry showed slight temporal variation, with more positive values in PC2 in the spring than in the fall (SD of 2.9 and 4.8 for PC1 and PC2, respectively).

5.2.2 Star West Upper

Water sources were similarly grouped as precipitation (rain and snow), hillslope groundwater (soil water, toe slope water, and upper hillslope water), and riparian water (Figure 6a). Bedrock groundwater samples were collected from a lower elevation in

275 the watershed and may not be representative of higher elevation groundwater signatures; therefore, they were excluded as a source at the upper sites. Precipitation clustered tightly in one location except for a couple samples of snow and rain, which increased the SD for precipitation (SD of 2.7 and 2.3 for PC1 and PC2, respectively). All sources showed similar variation as precipitation; hillslope groundwater had a SD of 4.3 and 2.7 for PC1 and PC2, respectively and riparian water had a SD of 3.0 and 2.0 for PC1 and PC2, respectively. A temporal pattern was observed for hillslope water in which hillslope water became

280 less like precipitation from spring to fall (Figure 6b). Temporal variation was also observed across months for riparian water, in which SO_4^{2-} concentrations increased from spring to fall (Figure 6b).
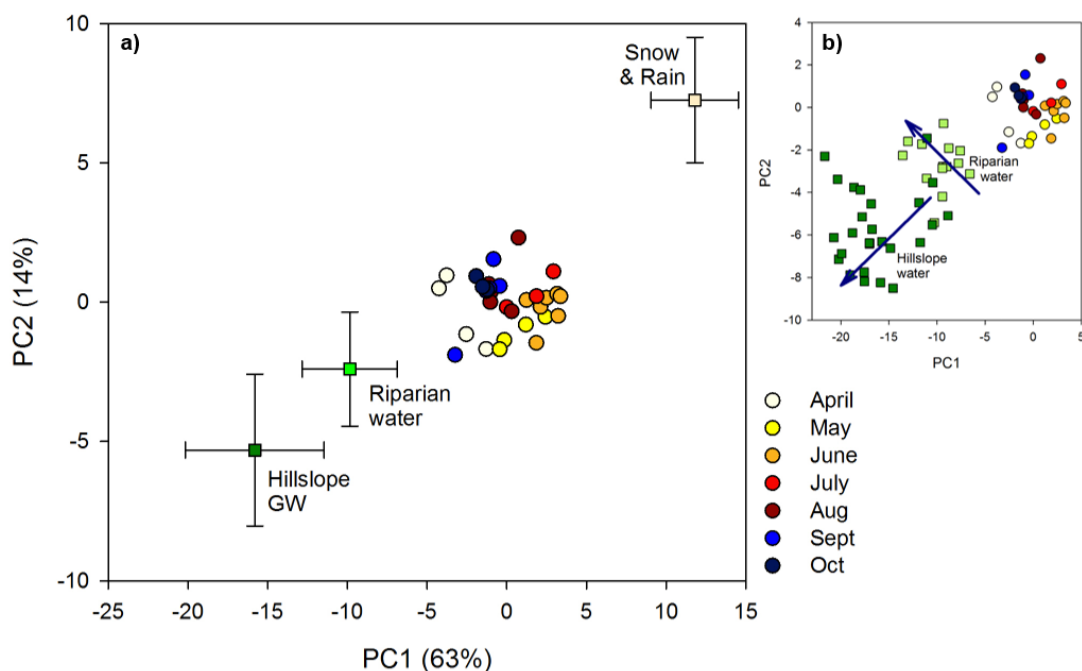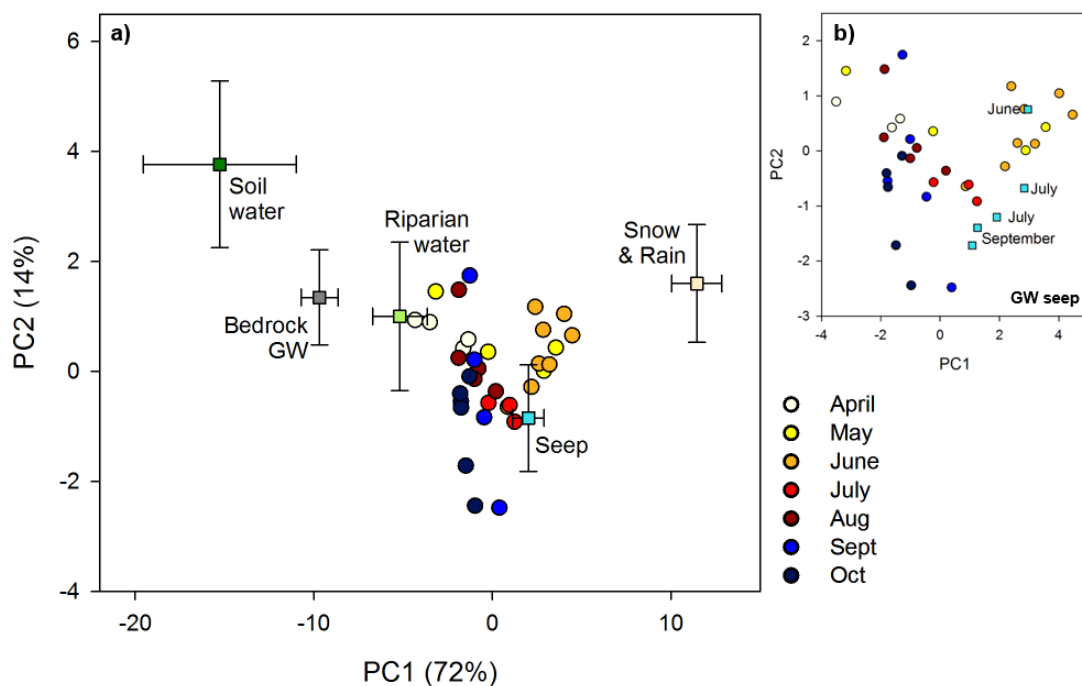

Figure 6: a) Star West Upper stream water chemistry from April to October in 2-D mixing space, which was derived from principal component analysis. Source water (precipitation, riparian water, and hillslope groundwater) was projected into the stream water

285 mixing space. PC1 and PC2 represent the first and second principal components, which explain 77 % of the variation in stream water. Error bars represent the standard deviation of the source waters for PC1 and PC2; b) shows the variation in riparian water and hillslope water samples from spring to fall (direction of arrows).

5.2.3 Star East Lower

Water sources were grouped as precipitation (snow and rain), soil water, riparian water, groundwater seep and bedrock
290 groundwater (Figure 7a). Precipitation and bedrock sources were the same as those used in SWL. Again, precipitation was
tightly clustered in the PCA biplot for SEL (SD of 1.4 and 1.1 for PC1 and PC2, respectively). Hillslope groundwater samples
were initially grouped together as a single source but high standard deviations and clustering within the group suggested the
separation of riparian water (SD of 1.0 and 1.5 for PC1 and PC2, respectively) and soil water (SD of 4.3 and 1.5 for PC1 and
PC2, respectively) as individual sources. Soil water was most different from stream water and varied from spring to fall
295 (increased Ca^{2+} and Mg^{2+} concentrations). Riparian water was most similar to stream water and did not vary over the season.
Bedrock groundwater was clustered in a linear pattern, but no temporal variation was observed. A single groundwater seep
that was chemically similar to stream water but temperatures were consistently cool was retained to aid in the explanation of
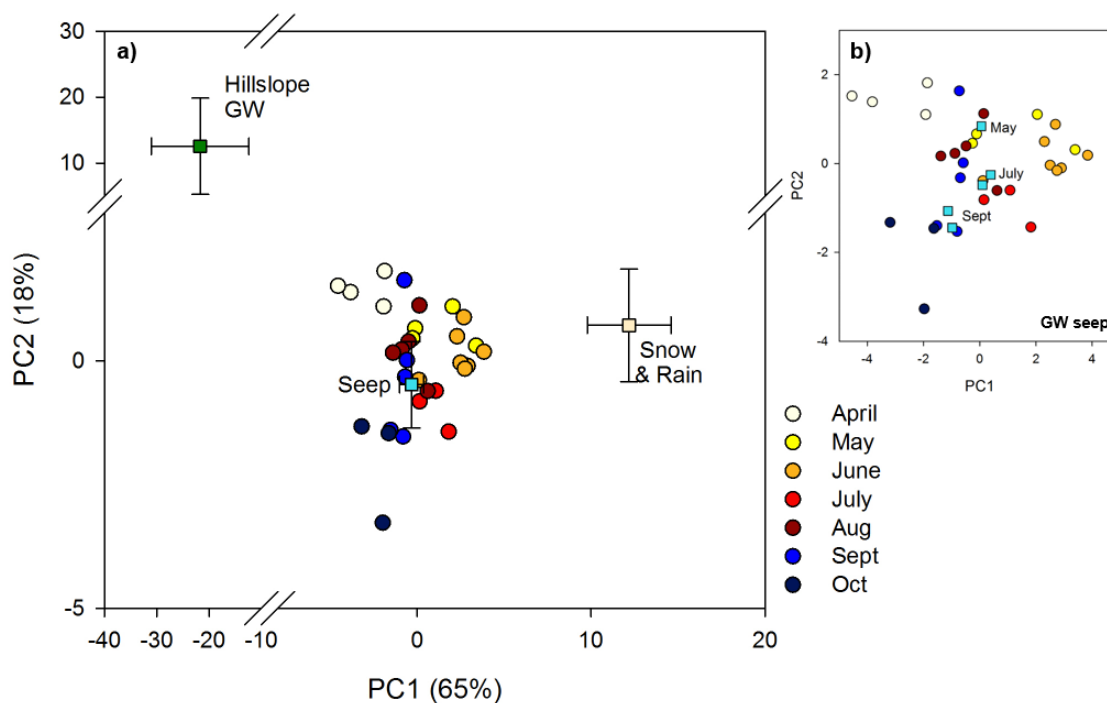stream water dynamics (Figure 7b).

300 **Figure 7: Star East Lower stream water chemistry from April to October in 2-D mixing space, which was derived from principal component analysis. Source water (precipitation, soil water, riparian water and bedrock groundwater) was projected into the stream water mixing space. PC1 and PC2 represent the first and second principal components, which explains 86 % of the variation in stream water. Error bars represent the standard deviation of the source waters for PC1 and PC2; b) shows the variation in the groundwater seep from June to September.**

5.2.4 Star East Upper

Water sources were grouped as precipitation (rain and snow), hillslope groundwater (soil water, riparian water, and toe slope water), and groundwater seep (Figure 8a). Precipitation was clustered in a linear pattern (SD of 2.4 and 1.1 for PC1 and PC2, respectively) but did not vary temporally. Large variation was observed for hillslope groundwater (SD of 9.3 and 7.3 for PC1 and PC2, respectively). Toe slope water and riparian water had some chemical dissimilarities but were not different enough from each other, or soil water, to be considered as different groups. No temporal pattern was observed for toe slope water or riparian water chemistry. Soil water varied temporally where it was more similar to riparian water and stream water in the spring and less like all stream water and all other samples (higher concentrations of ions) in the fall. As in SEL, a single groundwater seep that was chemically similar to stream water but temperatures were consistently cool was retained to aid in the explanation of stream water dynamics (Figure 8b).

Figure 8: Star East Upper stream water chemistry from April to October in 2-D mixing space, which was derived from principal component analysis. Source water (precipitation, hillslope groundwater, and groundwater seep) was projected into the stream water mixing space. PC1 and PC2 represent the first and second principal components, which explains 83 % of the variation in stream water. Error bars represent the standard deviation of the source waters for PC1 and PC2; b) shows the variation in the groundwater seep from May to September.

5.3 Stream water characterization

Stream water chemistry for all four sites showed temporal variation throughout the months of open-water flow but little variation between years. As a result, the temporal pattern of stream water was characterized for each site in general for both 2014 and 2015 combined. Further, due to the lack of source water samples during winter months, the temporal pattern of

325   stream water was characterized from April to October, which represents the dynamic hydrologic period from the beginning of snowmelt through to the start of the next year's snow accumulation period.

5.3.1 Star West Lower

PCA analysis indicated that 87 % of the variation in the data was explained by the first two PCs. Stream water samples were contained within an outer boundary created by source water when the temporal variation in source water was considered, but

330   not if mean values of source water were considered (Figure 5). In April, stream water was most similar to the hillslope groundwater. Stream water transitioned through May to become most similar to precipitation source water in June. In July, stream water was slightly more similar to hillslope groundwater and bedrock groundwater. In August, September and October, stream water chemistry was more variable and was similar to precipitation and hillslope and bedrock groundwater. The temporal pattern associated with stream water variation through the fall was perpendicular to the direction of the bedrock

335   temporal pattern, suggesting that hillslope groundwater, rather than bedrock groundwater, was driving stream water chemistry in the fall.

5.3.2 Star West Upper

PCA analysis indicated that 77 % of the variation in the data was explained by the first two PCs (Figure 6a). Sources formed two ends of a spectrum for stream water mixing rather than a triangle or polygon defining the mixing space. It is possible that

340   a source was missed in the sampling campaign but when the variation in sources was considered, the stream water was bounded by the two points. In April, stream water was most similar to hillslope groundwater and riparian water. Stream water transitioned through May and was more similar to precipitation in June and July. Stream water was similar to hillslope groundwater again through August, September, and October, but did not follow the same pathway as in the early summer months. These temporal differences in stream water between spring and fall are similar to the temporal differences observed

345   in riparian water from April to October rather than hillslope water (Figure 6b). It is likely that there was mixing between riparian water and stream water producing a similar temporal variation in their chemical signature.

5.3.3 Star East Lower

PCA analysis indicated that 86 % of the variation in the data was explained by the first two PCs (Figure 7a). Stream water samples were mostly contained within an outer boundary created by source water when the temporal variation in source water

350   was considered with the exception of September/October stream water, which plotted outside this boundary. In April, stream

water was most similar to the hillslope or bedrock groundwater. Stream water transitioned through May and was most similar to precipitation in June. In July and August, stream water became dissimilar from precipitation and was once again similar to riparian water or bedrock groundwater. In September and October, stream water was less similar to riparian water and plotted outside the boundary created by the identified sources. Since stream water was not contained within the boundary created by

355 the source water, it is likely that a source was missed from the analysis. The temporal variation in the groundwater seep followed the same pattern as the September/October stream water, suggesting the same source water for the groundwater seep and late fall baseflow (Figure 7b). Consistently cool temperatures of the seep (2.2-3.7 °C) suggest a deeper groundwater source.

5.3.4 Star East Upper

PCA analysis indicated that 83 % of the variation in the data was explained by the first two PCs (Figure 8a). Similar to SEL,

360 some of the stream water samples were outside the boundary formed by the stream water sources. In April, stream water was most similar to hillslope water. Stream water was similar to precipitation in May and June. In July and August, stream water was similar to hillslope groundwater but not as much as in April. In September and October, stream water became chemically dissimilar from all identified sources and plotted outside the boundary created by these sources. As in SEL, the temporal variation observed in the stream in September and October was also observed in the groundwater seep (spring to fall; Figure

365 8b). Again, it is likely that there was another source contributing to streamflow in the fall that was not captured by the field sampling. This was likely a deeper groundwater source due to consistently cool temperatures (2.5-3.5 °C) observed for the groundwater seep.

6 Discussion

6.1 Temporal and spatial variation in source water signatures

370 Chemical signatures of source water have been shown to vary seasonally and annually (Rademacher et al., 2005) as well as spatially across sub-watersheds (James and Roulet, 2006). As a result, James and Roulet (2006) suggested that only source water from within individual sub-watersheds of interest should be used in un-mixing calculations. Inamdar et al. (2013) further argued that mixing proportions should not be calculated because multiple assumptions are often violated and can lead to significant errors in un-mixing proportions. Rather, temporal and spatial variation in stream water and source water should be

375 examined and used to describe or to develop a physically-based conceptualization of runoff mechanisms.

Two of the key assumptions for EMMA, the chemical composition of sources does not change over 1) the time scale considered or 2) with space (Hooper, 2003; Inamdar, 2011), were violated in this dataset. Source water chemistry varied greatly across the watersheds. For example, when all hillslope samples from each sub-watershed were projected into the mixing space created by stream water at the watershed outlet (SM), large variability was evident between sites (Figure 9). While there was some

380 overlap between some sites (SWL and SEU), SWU was clearly different than the other hillslope samples. As a result, source water from within individual sub-watersheds was used to reduce the uncertainty associated with large spatial variability in

source water chemistry. However, the variability within sites was also quite large. The coefficient of variation (CV) of source

water was often larger than the CV of the stream water (there should be little to no variation in source water over time; James

and Roulet, 2006; Inamdar, 2011), particularly for K^+. The occasions where source water CV were smaller than stream water

385   CV for most ions were for seeps in SEU and SEL, bedrock groundwater in SWL and SEL, and hillslope and riparian water in
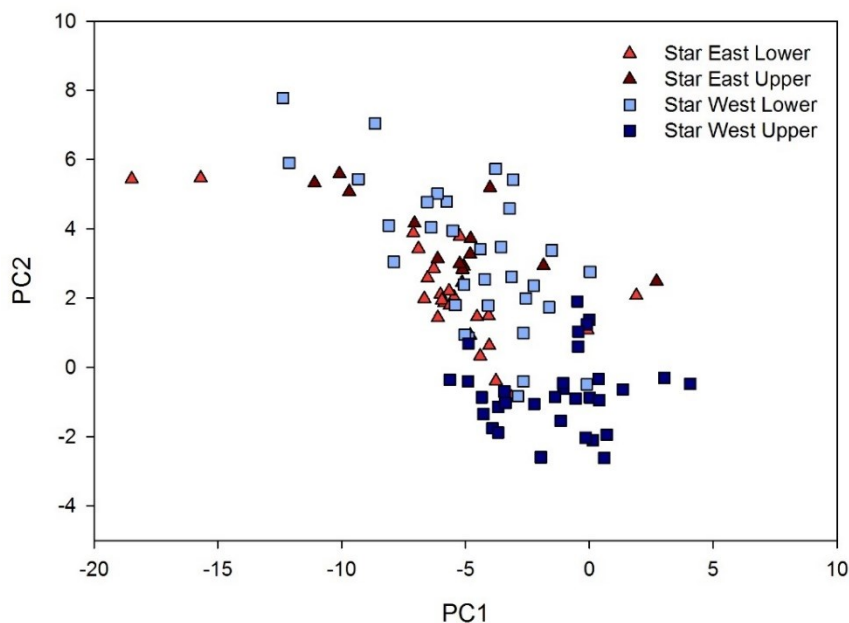
SWU.

Figure 9: Hillslope groundwater from all sub-watershed sites in 2-D mixing space, which was derived from principal component analysis of Star Main (Figure 1) stream water. PC1 and PC2 represent the first and second principal components

390   Despite the violation of assumptions, interesting and interpretable temporal trends in source water chemistry were observed.

For example, temporal variations in riparian water in SWU were observed from spring to fall and followed the same pattern

observed in stream water chemistry in May compared to September/October (Figure 6b). It is not clear if the stream chemistry

responded to variation in riparian chemistry or if riparian water responded to stream chemistry, but these pools of water were

likely mixing to create the same temporal pattern rather than the variation in hillslope water chemistry influencing the stream.

395   Other studies have also shown the importance of the riparian zone for "buffering" water chemistry and influencing stream

water contributions, although often at the event scale (McGlynn and Seibert, 2003; Grabs et al., 2012). Spencer et al. (2019)

presented water table dynamics in hillslope groundwater wells and suggested that the upper hillslope and the stream were only

connected during the spring freshet. This would suggest that hillslope water chemistry should reflect the dilution from

snowmelt and the subsequent drying of the hillslope, which should increase the concentration of water held in the soil from

400   spring to fall. The corresponding temporal pattern in hillslope water chemistry was observed in SWU (Figure 6b) and for soil

water chemistry in SEL and SEU.

Bedrock groundwater was consistent between years, but there is uncertainty around the variability of bedrock groundwater across the watershed. Although most of the stream is situated within the same geologic formation, there may be differences in bedrock groundwater chemistry associated with heterogeneous sedimentary layers or contact time (Freeze and Cherry, 1979).

405 Groundwater seeps that were sampled along the stream length could be used as a potential indicator of groundwater variability because they may flow through various formations or flow pathways. Temperature signals from seeps suggested some were groundwater-fed (consistent cool temperatures) and others were fed by shallow subsurface water (larger fluctuations in temperature; Taniguchi, 1993). However, ion concentrations of the seeps were not chemically distinct because they were generally similar to stream water or hillslope groundwater. This suggests that there are likely many complex subsurface flow

410 pathways making it difficult to differentiate between subsurface sources. Other tracers such as oxygen and hydrogen isotopes or non-conservative tracers such as nitrogen and dissolved organic carbon may help to better differentiate between seeps, hillslope groundwater, and bedrock groundwater (e.g., Cowie et al., 2017; Ali et al., 2010; Orlova and Branfireun, 2014). More wells in the bedrock and till are also required to characterize the variability in groundwater more robustly across the watershed (Rinderer et al., 2014) and improve the EMMA results.

415 **6.2 Temporal variation in stream water contributions**

Stream water contributions can be generalized for all sub-watersheds in a number of ways. The water that was stored in the hillslope was likely the first to reach the stream in the early spring prior to high flow as snowmelt started to saturate the landscape. The delivery of old water to the stream at the onset of snowmelt is similar to the flushing mechanism observed in the Turkey Lakes Watershed in central Ontario, Canada (Creed and Band, 1998) where high nitrogen concentrations were

420 observed prior to peak streamflow. McGlynn et al. (1999) also observed the displacement of old water to the stream at the onset of snowmelt in Sleepers River Research Watershed in Vermont, USA and suggested this was due to a small volume of snowmelt being added to a large storage of water already in the subsurface. This initial displacement of old water was likely followed by a dilution effect, where large volumes of low concentration snowmelt mixed with soil water and contributed to streamflow. Snowmelt was the major event that produced a water table response in all wells and connected the hillslopes to

425 the stream (Spencer et al., 2019). The initial snowmelt period was also the only time overland flow was observed at the study site. Other studies have also reported that snowmelt creates a dilution response in the stream (Rademacher et al., 2005; Cowie et al., 2017). Conversely, the opposite has also been observed whereby a previously disconnected source was connected to the stream and caused an increase in solute concentrations (McNamara et al., 2005). Although this was the main period of hydrologic connectivity in Star Creek, we did not observe the increase in stream water chemistry associated with newly

430 connected sources.

Stream water contributions were more similar within Star East (SEL and SEU) and Star West (SWL and SWU) sub-watersheds than between alpine/sub-alpine (SEU and SWU) and upper montane (SEL and SWL) sub-watersheds. PCA plots for SEL and SEU showed that stream water was most like precipitation in May and June, whereas this dilution effect occurred in June and July in SWL and May to July in SWU. The delayed response in SWL and SWU is consistent with the watershed storage

435   estimates from baseflow recession analysis (Spencer et al., 2019) that suggested that the west fork sub-watersheds had a larger
storage capacity than the east fork sub-watersheds. Accordingly, more water would be required to fill storage before saturation
or hydrologic connectivity occurred.

Differences in the east and west forks were also evident later in the year. In SWL and SWU, stream water was chemically
similar to hillslope groundwater in the fall (Figures 5 and 6a). In SEL and SEU, stream water was similar to hillslope

440   groundwater in August but fell outside the boundaries created by the identified sources in September and October (Figures 7a
and 8a). A groundwater seep in SEL and SEU followed similar temporal patterns as stream water from spring to fall (Figures
7b and 8b) and may provide insights into the sources of stream water in the fall. Consistently cool temperatures of the
groundwater seeps suggest they have a deeper bedrock groundwater source different than the bedrock groundwater well. Star
Creek has spatially heterogenous surficial deposits and geology (AGS, 2004) which likely has a large influence on groundwater

445   chemistry throughout the watershed. It is possible, therefore, that additional bedrock groundwater sources were contributing
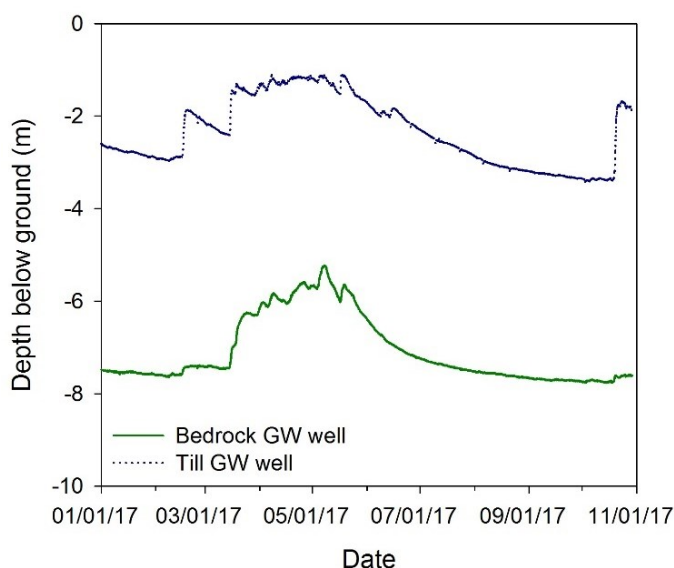to streamflow in Star Creek.

Topographic transitions and convergent zones have been associated with groundwater contributions to streamflow (Covino
and McGlynn, 2007; Hjerdt et al., 2004). While minimal groundwater discharge occurred over the mountain front recharge
zone in Humphrey Creek, southwest Montana, USA, considerable groundwater discharge was observed in the valley bottoms

450   (Covino and McGlynn, 2007). Large increases in the concentration of stream water ions that may be associated with strong
groundwater upwelling were not evident between April and October or along the length of the stream. However, chemical
signatures of groundwater seeps suggest that some bedrock groundwater may not be distinguishable from stream water.
Consequently, these transitions may not be visible in water chemistry along the length of the stream.

Although contamination of the till groundwater well has limited the inferences that could be made from water chemistry, water

455   levels in the bedrock and till groundwater wells do provide some insights into their contributions to streamflow. The till
groundwater well showed consistently slower recession curves compared to the bedrock groundwater well (Figure 10). Similar
to the post-glacial landscape in Sleepers River watershed (Shanley et al. 2015), slower drainage from till groundwater may be
partly responsible for maintaining streamflow during late summer. Heterogeneous glacial till deposits with different physical
characteristics were also linked to the variable release of stored water, and thus the variability in baseflow, in the Scottish

460   Highlands (Blumstock et al., 2015). Glacial till in the Rocky Mountains can be spatially heterogenous and likely has multiple
flow pathways within it (Langston et al., 2011). Clay lenses can create perched water tables that have different response times
than the rest of the till matrix (Evans et al., 2000) or create complex groundwater flow pathways (Freeze and Witherspoon,
1967).

The complexity in subsurface flow pathways that appears to influence runoff generation in Star Creek watershed may be

465   important in evaluating watershed resilience to disturbance. Primarily vertical percolation or groundwater recharge (Spencer
et al., 2019) and delayed or variable release of stored water could mute the impact of disturbance on peak flows. However,
excess water associated with forest disturbance would infiltrate into the subsurface, which may subsequently increase
baseflows. Star Creek sub-watersheds have a large storage capacity (300-450 mm) in glacial till and fractured bedrock (Spencer

Hydrology and
Earth System
Sciences
Discussions

et al., 2019). When compared to average annual precipitation (950 mm), it is possible that storage can mitigate the effects of
470   the increased net precipitation reaching the ground following disturbance by temporarily holding and slowly releasing the
excess water. Harder et al. (2015) also postulated that complex subsurface flow pathways and large storage capacity may be
partly responsible for the resiliency observed in Marmot Creek watershed (Alberta, Canada) following disturbance; however,
more research is needed to determine the influence of disturbance on groundwater.

475   **Figure 10: Bedrock groundwater and till groundwater well responses (depth below ground, m) over the 2017 calendar year. Till
groundwater is more responsive but has slower recession slopes in the summer.**

7 Conclusions

Stream and source water chemistry in four sub-watersheds of Star Creek showed that Star East (SEL and SEU) and Star West
(SWL and SWU) sub-watersheds were more similar than alpine/sub-alpine (SEU and SWU) and upper-montane (SEL and
480   SWL) physiographic zones. PCA plots were used to conceptualize runoff generation. In general, old water reached the stream
first at the onset of spring melt in all sub-watersheds. This was followed by a dilution effect as the snowmelt saturated the
landscape and the hillslope was connected to the stream. Fall baseflows differed between Star East and Star West forks. Star
West stream water was once again similar to hillslope water, but Star East was unlike all measured sources. Slower recession
rates (and likely lower hydraulic conductivity) in the till groundwater well than in the bedrock groundwater well suggest that
485   water recharged into the till groundwater may be slowly released to the stream, thereby muting the effects of disturbance on
peak flows. While this large storage zone may be an important factor in watershed resilience to disturbance that has been
observed in front-range Rocky Mountain watersheds in Alberta, the influence of disturbance on groundwater dynamics is not
well understood. More research on the variability of bedrock and till groundwater chemistry is needed to clarify the difference
between these sources and their contributions to streamflow throughout the year.

Hydrology and
Earth System
Sciences
Discussions

Author contributions

US and AEA secured funding enabling this research and supervised the research project. SS designed and carried out the field research. SS analysed and interpreted the data with assistance from all co-authors, particularly ALC with statistics and R code. SS prepared the original draft of the manuscript with contributions in review and editing from all co-authors.

Data availability

Please contact the corresponding author for data availability.

Competing interests

The authors declare no conflicts of interest.

References

AGS, Alberta Geologic Survey: Bedrock geology of Alberta (GIS data), http://www.ags.gov.ab.ca, 2004.

Ali, G. A., Roy, A. G., Turmel, A-C, and Courchesne, F.: Source-to-stream connectivity through end-member mixing analysis, J. Hydrol., 392, 119–135, doi:10.1016/j.jhydrol.2010.07.049, 2010.

Andres, D., Van Der Vinne, G., and Sterenberg, G.: Hydrologic, hydrogeologic, thermal, sediment and channel regimes of the Tri-Creeks experimental Basin, Alberta Research Council, Edmonton, AB, Rep. No. SWE-87/01. Vol. 1. 418 pp, 1987.

Barthold, F. K., Tyralla, C., Schneider, K., Vaché, K. B., Frede, H. G., and Breuer, L.: How many tracers do we need for end member mixing analysis (EMMA)? a sensitivity analysis, Water Resour. Res., 47 (8), 1–14, doi:10.1029/2011WR010604, 2011.

Blumstock, M., Tetzlaff, D., Malcolm, I. A., Neutzmann, G., and Soulsby, C.: Baseflow dynamics: Multi-tracer surveys to assess variable groundwater contributions to montane streams under low flows, J. Hydrol., 527, 1021–1033, doi:10.1016/j.jhydrol.2015.05.019, 2015.

Burns, D. A., Murdoch, P. S., Lawrence, G. B., and Michel, R. L.: Effect of groundwater springs on NO_3^- concentrations
520 during summer in Catsill Mountain streams, Water Resour. Res., 34 (8), 1987–1996, 1998.

Boon, S.: Snow accumulation following forest disturbance, Ecohydrology, 5 (3), 279–285, doi:10.1002/eco.212, 2012.

Brown, A. E., Zhang, L., McMahon, T. A., Western, A. W., and Vertessy, R. A.: A review of paired catchment studies for determining changes in water yield resulting from alterations in vegetation, J. Hydrol., 310 (1–4), 28–61, doi:10.1016/j.jhydrol.2004.12.010, 2005.

525 Burles, K., and Boon, S.: Snowmelt energy balance in a burned forest plot, Crowsnest Pass, Alberta, Canada, Hydrol. Process. 25 (19), 3012–3029, doi:10.1002/hyp.8067, 2011.

Christophersen, N., and Hooper, R. P.: Multivariate analysis of stream water chemical data: the use of principal components analysis for the end-member mixing problem, Water Resour. Res., 28 (1), 99–107, doi:10.1029/91WR02518, 1992.

Covino, T. P., and McGlynn, B. L.: Stream gains and losses across a mountain-to-valley transition: impacts on watershed
530 hydrology and stream water chemistry, Water Resour. Res., 43, W10431, doi:10.1029/2006WR005544, 2007.

Cowie, R. M., Knowles, J. F., Dailey, K. R., Williams, M. W., Mills, T. J., and Molotch, N. P.: Sources of streamflow along a headwater catchment elevational gradient, J. Hydrol., 549, 163–178, doi:10.1016/j.hydrol.2017.03.044, 2017.

Creed, I. F. and Band L. E.: Export of nitrogen from catchments with a temperate forest: evidence for a unifying mechanism regulated by variable source area dynamics, Water Resour. Res., 34 (11), 3105-3120, 1998.

535 Creed, I. F., Sass, G. Z., Buttle, J. M., and Jones, J. A.: Hydrological principles for sustainable management of forest ecosystems, Hydrol. Process., 25, 2152–2160, doi:10.1002/hyp.8056, 2011.

Dahlke, H. E., Easton, Z. M., Lyon, S. W., Walter, M. T., Destouni, G., and Steenhuis, T. S.: Dissecting the variable source area concept – subsurface flow pathways and water mixing processes in a hillslope, J. Hydrol., 420, 125–141, doi:10.1016/j.hydrol.2011.11.052, 2012.

540 Dixon, D., Boon, S., and Silins, U.: Watershed-scale controls on snow accumulation in a small montane watershed, southwestern Alberta, Canada, Hydrol. Process., 28, 1294–1306, doi:10.1002/hyp.9667, 2014.

Evans, J. E., Prepas, E. E., Devito, K. J., and Kotak B. G.: Phosphorus dynamics in shallow subsurface waters in an uncut and cut subcatchment of a lake on the Boreal Plain, Can. J. Fish. Aquat. Sci., 57 (Suppl. 2), 60–72, 2000.

Floriancic, M. G., van Meerveld, I., Smoorenburg, M., Margreth, M., Naef, F., Kirchner, J. W., and Molnar, P.: Spatio-temporal
545 variability in contributions to low flows in the high Alpine Poschiavino catchment, Hydrol. Process., 32 (26), 3938–3953, doi:10.1002/hyp.13302, 2018.

Freeze, R. A., and Cherry J. A. (Eds.): Groundwater, Prentice-Hall, New Jersey, USA, 1979.

Freeze, R. A., and Witherspoon P. A.: Theoretical analysis of regional groundwater flow 2. Effect of water-table configuration and subsurface permeability variation., Water Resour. Res., 3 (2), 623–634, 1967.

Hydrology and
Earth System
Sciences
Discussions

550   Goodbrand, A. and Anderson, A.: Hydrologic resilience of a Canadian Foothills watershed to forest harvest. EGU General
Assembly, Vienna, Austria, 17–22 April 2016, EGU2016-10932, 2016.

Grabs, T., Bishop, K., Laudon, H., Lyon, S. W., and Seibert, J.: Riparian zone hydrology and soil water total organic carbon
(TOC): implications for spatial variability and upscaling of lateral riparian TOC exports, Biogeosciences, 9, 3901–3916,
doi:10.5194/bg-9-3901-2012, 2012.

555   Harder, P., Pomeroy, J. W., and Westbrook, C. J.: Hydrological resilience of a Canadian Rockies headwaters basin subject to
changing climate, extreme weather, and forest management, Hydrol. Process., 29, 3905–3924, doi:10.1002/hyp.10596, 2015.

Hjerdt, K. N., McDonnell, J. J., Seibert, J., and Rodhe, A.: A new topographic index to quantify downslope controls on local
drainage, Water Resour. Res., 40, W05602, doi:10.1029/2004WR003130, 2004.

Hood, J. L., and Hayashi, M.: Characterization of snowmelt flux and groundwater storage in an alpine headwater basin, J.
560   Hydrol., 521, 482–497, doi:10.1016/j.hydrol.2014.12.041, 2015.

Hooper, R. P.: Diagnostic tools for mixing models of stream water chemistry, Water Resour. Res., 39 (3), 1055,
doi:10.1029/2002WR001528, 2003.

Inamdar, S.: The use of geochemical mixing models to derive runoff sources and hydrologic flow paths, in: Forest hydrology
and biogeochemistry: synthesis of past research and future directions, edited by: Levia, D. F., Carlyle-Moses, D., and Tanaka,
565   T., Springer, New York, USA, 163–183, doi:10.1007/978-94-007-1363-5, 2011.

Inamdar, S., Dhillon, G., Singh, S., Dutta, S., Levia, D., Scott, D., Mitchell, M., Van Stan, J., and McHale, P. Temporal
variation in end-member chemistry and its influence on runoff mixing patterns in a forested, Piedmont catchment, Water
Resour. Res., 49 (4), 1828–1844, doi:10.1002/wrcr.20158, 2013.

James, A. L., and Roulet, N. T.: Investigating the applicability of end-member mixing analysis (EMMA) across scale: a study
570   of eight small, nested catchments in a temperate forested watershed, Water Resour. Res., 42 (8), 1–17,
doi:10.1029/2005WR004419, 2006.

Johannessen, M., and Henriksen, A.: Chemistry of snow meltwater: changes in concentration during melting, Water Resour.
Res., 14 (4), 615–619, 1978.

Langston, G., Bentley, L. R., Hayashi, M., McClymont, A., and Pidlisecky, A.: Internal structure and hydrological functions
575   of an alpine proglacial moraine, Hydrol. Process., 25, 2967–2982, doi:10.1002/hyp.8144, 2011.

Liu, F., Williams, M. W., and Caine, N.: Source waters and flow paths in an alpine catchment, Colorado Front Range, United
States, Water Resour. Res., 40, W09401, doi:10.1029/2004WR003076, 2004.

McClymont, A. F., Hayashi, M., Bentley, L. R., Muir, D., and Ernst, E.: Groundwater flow and storage within an alpine
meadow-talus complex, Hydrol. Earth Syst. Sc., 14 (6), 859–872, 2010.

580   McGlynn, B. L., McDonnell, J. J., Shanley, J. B., and Kendall, C.: Riparian zone flowpath dynamics during snowmelt in a
small headwater catchment, J. Hydrol., 222 (1–4), 75–92, doi:10.1016/S0022-1694(99)00102-X, 1999.

McGlynn, B. L., and Seibert, J.: Distributed assessment of contributing area and riparian buffering along stream networks,
Water Resour. Res., 39 (4), 1082, doi:10.1029/2002WR001521, 2003.

McNamara, J. P., Chandler, D., Seyfried, M., and Achet, S.: Soil moisture states, lateral flow, and streamflow generation in a

585 semi-arid, snowmelt-driven catchment, Hydrol. Process, 19 (20), 4023–4038, doi:10.1002/hyp.5869, 2005.

Orlova, J., and Branfireun, B. A.: Surface water and groundwater contributions to streamflow in the James Bay Lowland, Canada, Arct. Antarct. Alp. Res., 46 (1), 236–250, doi:10.1657/1938-4246-46.1.236, 2014.

Pfister, L., Martínez-Carreras, N., Hissler, C., Klaus, J., Carrer, G. E., Stewart, M. K., and McDonnell, J. J.: Bedrock geology controls on catchment storage, mixing, and release: a comparative analysis of 16 nested catchments, Hydrol. Process., 31,

590 1828–1845, doi:10.1002/hyp.11134, 2017.

Pulley, S., and Collins, A. L.: Tracing catchment fine sediment sources using the new SIFT (SedIment Fingerprinting Tool) open source software, Sci. Total Environ., 635, 838–858, doi:10.1016/j.scitotenv.2018.04.126, 2018.

Pulley, S., Foster, I., and Antunes, P. The uncertainties associated with sediment fingerprinting suspended and recently deposited fluvial sediment in the Nene river basin, Geomorphology, 228, 303–319, doi:10.1016/j.geomorph.2014.09.016,

595 2015.

R Core Team: R: A language and environment for statistical computing. R Foundation for Statistical Computing, Vienna, Austria. URL: http://www.R-project.org/, 2014.

Rademacher, L. K., Clark, J. F., Clow, D. W., and Hudson, G. B.: Old groundwater influence on stream hydrochemistry and catchment response times in a small Sierra Nevada catchment: Sagehen Creek, California, Water Resour. Res., 41 (2), 1–10,

600 doi:10.1029/2003WR002805, 2005.

Remenda, V. H., and van der Kamp, G.: Contamination from sand-bentonite seal in monitoring wells installed in aquitards, Groundwater, 35 (1), 39–46, 1997.

Rinderer, M., van Meerveld, H. J., and Seibert, J.: Topographic controls on shallow groundwater levels in a steep, prealpine catchment: when are the TWI assumptions valid?, Water Resour. Res., 50, 6067–6080, doi:10.1002/2013WR015009, 2014.

605 Scott, D. F.: The hydrological effects of fire in South African mountain catchments, J. Hydrol., 150, 409–432, doi:10.1016/0022-1694(93)90119-T, 1993.

Shanley, J. B., Sebestyen, S. D., McDonnell, J. J., McGlynn, B. L., and Dunne, T.: Water's Way at Sleepers River watershed–revisiting flow generation in a post-glacial landscape, Vermont USA, Hydrol. Process., 29 (16), 3447–3459, doi:10.1002/hyp.10377, 2015.

610 Silins, U., Stone, M., Emelko, M. B., and Bladon, K. D.: Sediment production following severe wildfire and post-fire salvage logging in the Rocky Mountain headwaters of the Oldman River Basin, Alberta, Catena, 79, 189–197, doi:10.1016/j.catena.2009.04.001, 2009.

Spencer, S. A., Silins, U., and Anderson A. E.: Precipitation-runoff and storage dynamics in watersheds underlain by till and permeable bedrock in Alberta's Rocky Mountains, Water Resour. Res., 55 (12), 10690–10706, doi:10.1029/2019WR025313,

615 2019.

Stednick, J. D.: Monitoring the effects of timber harvest on annual water yield, J. Hydrol., 176 (1–4), 79–95, doi:10.1016/0022-1694(95)02780-7, 1996.

Taniguchi, M.: Evaluation of vertical groundwater fluxes and thermal properties of aquifers based on transient temperature-depth profiles, Water Res., 29 (7), 2021–2026, 1993.

620   Uchida, T., McDonnell, J. J., and Asano, Y.: Functional intercomparison of hillslopes and small catchments by examining water source, flowpath and mean residence time, J. Hydrol., 327, 627–642, doi:10.1016/j.jhydrol.2006.02.037, 2006.

Varhola, A., Coops, N. C., Weiler, M., Moore, R. D.: Forest canopy effects on snow accumulation and ablation: an integrative review of empirical results, J. Hydrol., 392 (3–4), 219–233, doi:10.1016/j.jhydrol.2010.08.009, 2010.

Venables, W. N., and Ripley, B. D.: Modern applied statistics with S. Fourth Edition. Springer, New York, USA. ISBN 0-387-

625   95457-0, 2002.

Weihs, C., Ligges, U., Luebke, K., and Raabe, N.: klaR analyzing German business cycles, in: Data analysis and decision support, edited by: Baier, D., Decker, R., and Schmidt-Thieme, L., 335–343, Springer-Verlag, Berlin, Germany, 2005.

Williams, C., Silins, U., Bladon, K. D., Martens, A. M., Wagner, M. J., and Anderson, A.: Rainfall-runoff dynamics following wildfire in mountainous headwater catchments, Alberta, Canada, American Geophysical Union Fall Meeting, San Francisco,

630   USA, 14–18 December 2015, H34B-06, 2015.

Williams, C. H. S., Silins, U., Spencer, S. A., Wagner, M. J., Stone, M., and Emelko, M. B.: Net precipitation in burned and unburned subalpine forest stands after wildfire in the northern Rocky Mountains, Int. J. Wildland Fire., 28 (10), 750–760, doi:10.1071/WF18181, 2019.

Winkler, R., Spittlehouse, D., and Boon, S.: Streamflow response to clear-cut logging on British Columbia's Okanagan

635   Plateau, Ecohydrology, 10 (2), 1–15, doi:10.1002/eco.1836, 2017.